Nuclear Engineering and Technology 53 (2021) 3431–3437

Contents lists available at ScienceDirect

Nuclear Engineering and Technology

journal homepage: www.elsevier.com/locate/net

Original Article

Comparison of theoretical and machine learning models to estimate gamma ray source positions using plastic scintillating optical fiber detector

Jinhong Kim [a], Seunghyeon Kim [a], Siwon Song [a], Jae Hyung Park [a], Jin Ho Kim [a], Taeseob Lim [a], Cheol Ho Pyeon [b], Bongsoo Lee [a, *]

[a] School of Energy Systems Engineering, Chung-Ang University, Seoul, 06974, South Korea
[b] Research Center for Safe Nuclear System, Institute for Integrated Radiation and Nuclear Science, Kyoto University, Asashiro-nishi, Kumatori-cho, Sennan-gun, Osaka, 590-0494, Japan

ARTICLE INFO

Article history:
Received 23 February 2021
Received in revised form
13 April 2021
Accepted 15 April 2021
Available online 3 May 2021

Keywords:
Plastic scintillating optical fiber
Gamma ray detection
Position estimation
Machine learning
Nonlinear regression

ABSTRACT

In this study, one-dimensional gamma ray source positions are estimated using a plastic scintillating optical fiber, two photon counters and via data processing with a machine learning algorithm. A nonlinear regression algorithm is used to construct a machine learning model for the position estimation of radioactive sources. The position estimation results of radioactive sources using machine learning are compared with the theoretical position estimation results based on the same measured data. Various tests at the source positions are conducted to determine the improvement in the accuracy of source position estimation. In addition, an evaluation is performed to compare the change in accuracy when varying the number of training datasets. The proposed one-dimensional gamma ray source position estimation system with plastic scintillating fiber using machine learning algorithm can be used as radioactive leakage scanners at disposal sites.

1. Introduction

Currently, both high-level radioactive wastes (HLW) and large amounts of low-and-intermediate-level radioactive wastes (LILW) are generated from nuclear power plants as well as medical and industrial facilities. LILW can be classified into short, medium, and long-lived waste in accordance with its decay time. This waste is sealed in radwaste drums before disposal and one of the main issues has been monitoring the leakage of short-and-medium term radioactive isotopes since there is possibility of leakage due to the structural weakness or accident in radwaste drums. Scanning the drums with proper sensors that have rapid radioactive source position estimation capabilities can help quickly trace the location of any leak and reduce the risk of wider contamination to the environment as well as the operators [1,2].

Various methods of estimating the position of radioactive sources have been investigated and practically applied. One of the most prevalent and effective methods is the use of scintillation materials, which react with detectable radiation and emit visible light. Recently, plastic scintillating optical fiber (PSOF) has been used as a radioactive source position detector to scan radwaste drums, providing the position of the leakage and dose rate in real time [1,3,4]. PSOF is an organic scintillator-type radiation detector that also performs a light guide role, similar to conventional optical fiber [5,6]. PSOFs have several advantages over other conventional detecting materials, such as long length usability, flexibility, adaptable shape, high water resistance, stability in magnetic fields and inexpensive manufacturing costs. Conversely, PSOFs have relatively low light yield and sensitivity than common inorganic scintillators; however, the use of bundle-type PSOF detectors can offset these disadvantages [6–8,13,14].

Position estimation of gamma ray sources using a PSOF can be achieved via three methods. The two classical methods are the measurement of attenuated intensity of scintillation light and the measurement of pulse height difference. A more recent method is the measurement of signal-received time difference, which is possible owing to the development of high-performance signal acquisition equipment [5].

* Corresponding author.
E-mail address: bslee@cau.ac.kr (B. Lee).

https://doi.org/10.1016/j.net.2021.04.019

Measurement of signal-received time difference, also known as the time-of-flight (TOF) method, is based on the fact that the speed of a light signal remains constant within the scintillation materials. The time difference of signals received by light-measuring device located at each end of the PSOF is directly converted into the position of the source. Previous studies on estimating the position of gamma ray sources using PSOF detectors with the TOF method, include Nohtomi et al. [8], Soramoto et al. [9], Emoto et al. [10], Chichester et al. [11] and Gamo et al. [12]. Detection systems using the TOF method generally have a high accuracy and resolution. However, there is a high cost for the data acquisition equipment with a high sampling rate, which is necessary due to the short decay time of an organic scintillator such as PSOF.

Measurement of pulse height is mainly used for radionuclide identification and wide-area surveying [13,14]. Measuring the pulse at either end of the PSOF and calculating the ratio of pulse heights enables tracing of the location of the scintillation signals, because the pulse height is attenuated when it is transmitted through PSOF. Imai et al. [14] conducted an experiment using a PSOF detector and photomultiplier tubes to estimate the position of gamma ray sources by measuring the pulse height ratio. The main disadvantage of this method is that the accuracy of the estimated location can vary according to the position at which scintillation occurs. This is due to the transmission loss of the signal in PSOF and the quantum efficiency of the light-measuring device, which change with respect to the wavelength of the signal, resulting in a deviation of the pulse spectra from exponential attenuation [15].

Measurement of attenuated intensity of scintillation light is the simplest method and is based on the assumption that the signal attenuation due to the scintillating material is linear. One of the merits of this method is that the system components are relatively simple and inexpensive. However, the main disadvantage of this system is that the attenuation ratio of signal intensity and the photon detector efficiency both vary depending on the wavelength of the scintillation signal [15,16]. This results in an inaccurate estimation of the position of the source, as the change in the attenuation coefficient of the scintillation signal is a complex value and not a constant. Moreover, in the applicative area, an un-collimated radioactive source can decrease the accuracy of source position estimation. To solve the critical drawback of inaccuracy, it is essential to determine the nonlinear relationships between the signal intensity and resultant estimated position, rather than consider the regular relationships such as exponential, logarithmic, or linear.

One of the most widely used techniques to determine unknown and complicated relationships between various parameters obtained by experiments is the use of artificial intelligence (AI) algorithms, such as machine learning (ML) or artificial neural network (ANN) [17–19]. Several studies for detecting radiation using AI algorithms have been conducted and indicate the possibility of improvement in detection [20,21].

Table 1
Specific properties of BCF-12.

Properties	Value
Emission peak (nm)	435
Decay time (ns)	3.2
# of photons per MeV	~8000
Core refractive index	1.6
Cladding refractive index	1.49
Cladding type	Single cladding type
Diameter (mm)	3.0

In this study, the one-dimensional (1D) gamma ray source positions are estimated using a PSOF, two photon counters and via data processing using the ML algorithm. A nonlinear regression algorithm using the Keras framework in a Python environment is used to construct the ML model for position estimation of radioactive sources. The position estimation results using ML are compared with theoretical position estimation results based on the same measured data. Various tests are conducted to determine the improvement in accuracy of the source position estimation, and to compare the change in accuracy by varying the number of training datasets of the ML model.

2. Materials and methods

2.1. Materials

Typically, a PSOF consists of a central core surrounded by cladding. The base materials of both the core and cladding are polymeric materials such as polystyrene (PS), polyvinyl toluene (PVT), or polymethyl-methacrylate (PMMA). Organic fluorescent dyes are normally added to the base material of the core [5]. The difference between the refractive indices of the core and cladding enables total internal reflection of light within the core, resulting in the transmission of light signals to the end of the fiber. The PSOF used in this study is BCF-12 (Saint Gobain Crystals). BCF-12 is suitable for a one-dimensional detector to estimate gamma ray source positions due to its attenuation length and peak wavelength compared to those of other kinds of PSOFs which are commercially available. Table 1 lists the major specific properties of BCF-12 [22].

The photon counter used in this study is H11890-210 (Hamamatsu Photonics). Table 2 lists the major specific properties of H11890-210 [16].

Fig. 1 shows the experimental setup used to measure the scintillating light signals from a gamma ray source. A strand of BCF-12 PSOF with a length of 1 m is connected to photon counters at both ends. The customized connectors ensure the distance between the window of photon counter and PSOF is minimized. The photon counting data are directly transferred to the computer. The gamma ray source is positioned 5 cm below the PSOF and moved along the axis parallel to the PSOF. Measurements are not conducted at the 35 and 65 cm positions because of the location of the support bars that keep the PSOF in a straight line. The support bars are made of PMMA to prevent X-ray generations at the support bars.

For the experiment, Co-60 and Cs-137 gamma ray sources are used. A background count value is subtracted from the data in every measurement.

2.2. Theoretical method to estimate the position of source

Theoretical estimations of the 1D position of the gamma ray sources are derived from the photon counting data using the Beer-Lambert law of attenuation with several assumptions [23]. The attenuation coefficient is a specific property of the type of PSOF and is dependent on its diameter, the energy of the gamma radiation, and the number of photon counts corresponding to intensity, which is considered as the energy deposited by gamma rays.

From Fig. 2, the number of counted photons can be derived from equations (1) and (2), and by dividing equation (2) by equation (1), equation (3) is obtained as follows.

$$I_1 = I_0 e^{-\mu\left(\frac{L}{2}+x\right)} \tag{1}$$

Table 2
Specific properties of H11890-210.

Properties	Value
Spectral response (nm)	230–700
Peak sensitivity wavelength (nm)	400
Typical dark count (s^{-1})	50
Pulse-pair resolution (ns)	20
Effective area diameter	8

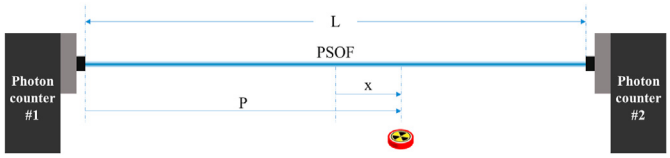

Fig. 2. Geometry schematics for estimating the position of source.

$$I_2 = I_0 e^{-\mu(\frac{L}{2}-x)} \tag{2}$$

$$\frac{I_2}{I_1} = e^{2\mu x} \tag{3}$$

where I_n is the light intensity measured at the nth photon counter, I_o is the initial (not attenuated) light intensity, μ is the attenuation coefficient of PSOF, L is the total length of the PSOF, and x is the position of the gamma ray source.

From equation (3), equations (4) and (5) are obtained. This proves that the 1D position of the gamma ray source can be obtained through theoretical estimations.

$$x = \frac{1}{2\mu}\ln\frac{I_2}{I_1} \tag{4}$$

$$P = \frac{L}{2} + x \tag{5}$$

where P is estimated position with zero point in one end of PSOF.

The value of the attenuation coefficient used to estimate the position of the gamma ray source theoretically can be derived experimentally, using the measured data with equation 6 derived from equations 4 and 5.

2.3. Machine learning model construction

To estimate the position regardless of the activity of the source, pre-processed photon counting data are used in ML. Using equations (7) and (8), the photon counting data are converted from absolute count values to relative count values.

$$RC_1 = \frac{C_1}{C_1 + C_2} \tag{7}$$

$$RC_2 = 1 - RC_1 = \frac{C_2}{C_1 + C_2} \tag{8}$$

where C_1 and C_2 are the number of photons counted by photon counters 1 and 2, respectively, and RC is the relative count.

For the construction of the position estimation model and evaluation process, the Keras framework is used with a Tensorflow back-end engine in a Python environment. The nonlinear regression method with a rectified linear unit activation function and Adam optimizer is used to construct the model [24,25]. Fig. 3 shows a detailed description of the ML model and the notation Pos corresponds to the position of the gamma ray source.

As shown in Fig. 3, the input data include RC_1, RC_2 and the actual position of the source in the training process. Two hidden layers exist with 64 nodes in each layer, and the source position is estimated in the output layer. During the training, the maximum epochs are set to 200, and 10% of the data are randomly separated from the training data at each epoch to be used as model validation data. The validation data are also used as the criterion for the early-stopping process, by which the process of constructing the ML model stops if the validation loss does not decrease anymore before the predetermined number of epochs is over. For the position estimation of Co-60 and Cs-137 sources, the ML model are made using Co-60 and Cs-137 training data, respectively. The ML models are evaluated using test data, which are measured separately from the training data without any change in the structure of the ML model.

2.4. Experimental data acquisition results

Table 3 lists the number of photon counting data per position for each radioactive source. A single datum corresponds to the number of photons measured in 10 s. The activities of Co-60 and Cs-137 were approximately 49 and 41 μCi, respectively. The number of photon counting data measured in 0.1 s is 100 and the accumulated values in 10 s are used as a single datum. The standard deviations of statistical fluctuation of counting data are in the ranges of 0.5~1.0%, 0.7~1.3% for Co-60 with 49 μCi and Cs-137 with 41 μCi, respectively, and the fluctuations of counting data can be negligible.

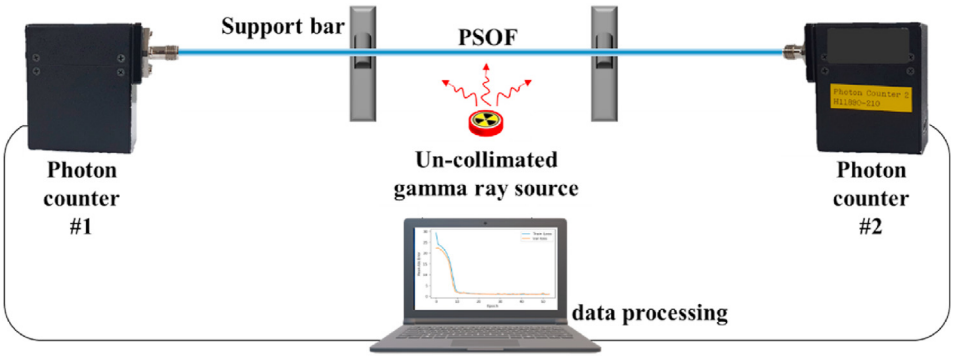

Fig. 1. Experimental setup.

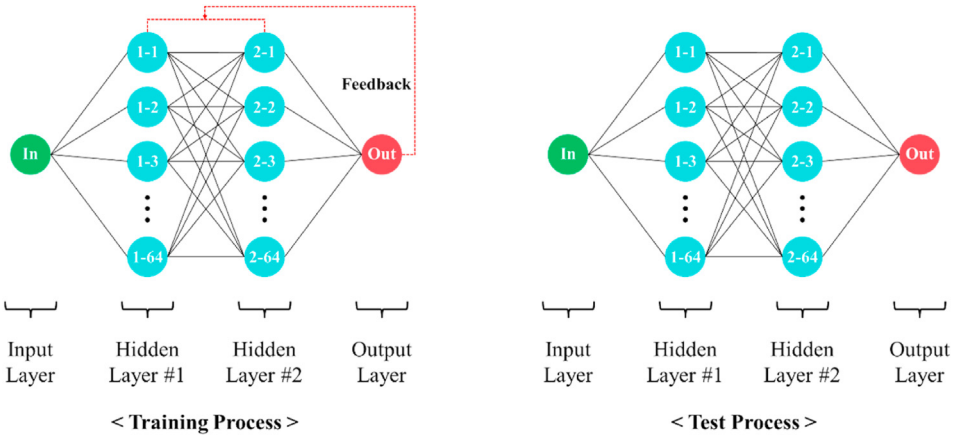

Fig. 3. Detailed description for ML model.

Table 3
Summary for the number of measured data and measured positions for ML model.

The number of training data per position	180
Total number of training data	1620
Measured position for training data (cm)	10, 20, 30, 40, 50, 60, 70, 80, 90
The number of test data per position	10
Total number of test data	180
Measured position for test data (cm)	10, 15, 17, 20, 25, 30, 40, 43, 45, 50, 55, 60, 70, 75, 78, 80, 85, 90

180 number of Co-60 and Cs-137 photon counting data per position are measured and used as training data for the position estimation models, and 10 number of Co-60 and Cs-137 photon counting data per position are measured and used as test data for the position estimation models. For the training data, the source positions are chosen at intervals of 10 cm from 10 to 90 cm along the PSOF. The test data source locations used the same positions as the training data, the central positions of the two adjacent training data excluding the location of support bars, and three irregular positions. The term regular position in this study is defined as all the positions of the test data except at positions 17, 43, and 78 cm. These three positions are categorized separately as randomly sampled test data. Table 3 lists the summary of the number of measured data and measured positions for the ML model.

The attenuation coefficients of PSOF for theoretical estimation are obtained experimentally using the training data and equation 6. The attenuation coefficients for Co-60 and Cs-137 model are 0.4457 m^{-1} and 0.3707 m^{-1}, respectively.

3. Experimental results

The ML position estimation results of gamma ray sources are compared to the theoretical position estimation results in various manners. First, the evaluation is conducted at the regular source positions to compare both accuracy and precision. Accuracy is evaluated through the overall error values, and precision is evaluated through the range of error bars. In this study, the error is defined as the absolute value of the difference between the estimated and the actual position, and the overall error is defined as the total average of errors at all measured positions.

Fig. 4 shows the comparative plots between the position estimation results using ML and theoretical estimations. In Fig. 4, the red dots show the actual positions as a reference, green dots show the results of theoretical estimations and blue dots show the results of position estimation using ML. The error bars indicate the boundary between the maximum and minimum estimated positions for both methods.

Fig. 5 shows the error plots for the ML model position estimation results and theoretical estimations. In Fig. 5-(a), the ML estimation results show lower error values at all regular positions. In Fig. 5-(b), the ML estimation result at the 25 cm position shows slightly higher error values of 0.25 cm, and the results at the rest positions show lower error values.

In addition, a test of the ML position estimation model with three randomly sampled positions (17, 43, and 78 cm) is conducted to identify whether the ML models are accurate with irregular data away from regular points. As shown in Fig. 6, the error values of the ML position estimation for both Co-60 and Cs-137 are lower than the theoretical estimation results at all random points verifying that the ML models for both sources are accurate at any position as well as at almost regular positions.

Table 4 lists estimated average positions and their standard deviations using ML and theoretical models for both Co-60 and Cs-137 sources. And, Table 5 lists the overall error values for both Co-60 and Cs-137 test results for position estimation models including test data at both regular and randomly sampled positions. In terms of overall error, the ML model results show approximately, an 91.54% improvement ratio (IR) in position estimation accuracy for Co-60 source, and a 77.12% IR for Cs-137 source compared to theoretical estimation. The value of IR is defined as equation (9) in this study.

$$\text{Improvement ratio (IR)} = \frac{E_T - E_M}{E_T} \tag{9}$$

where E_T is the error value from the theoretical estimation, and E_M is the error value from ML estimation.

To evaluate whether the test result is changed relative to the number of training datasets, various combinations of training datasets are used to construct ML models, and the evaluations for different types of model are performed. Model 1 uses the training data measured at three positions, that is, 10, 50, and 90 cm. Model 2 uses the training data obtained at five positions, that is, 10, 30, 50, 70, and 90 cm. Model 3 uses all of the training data measured at

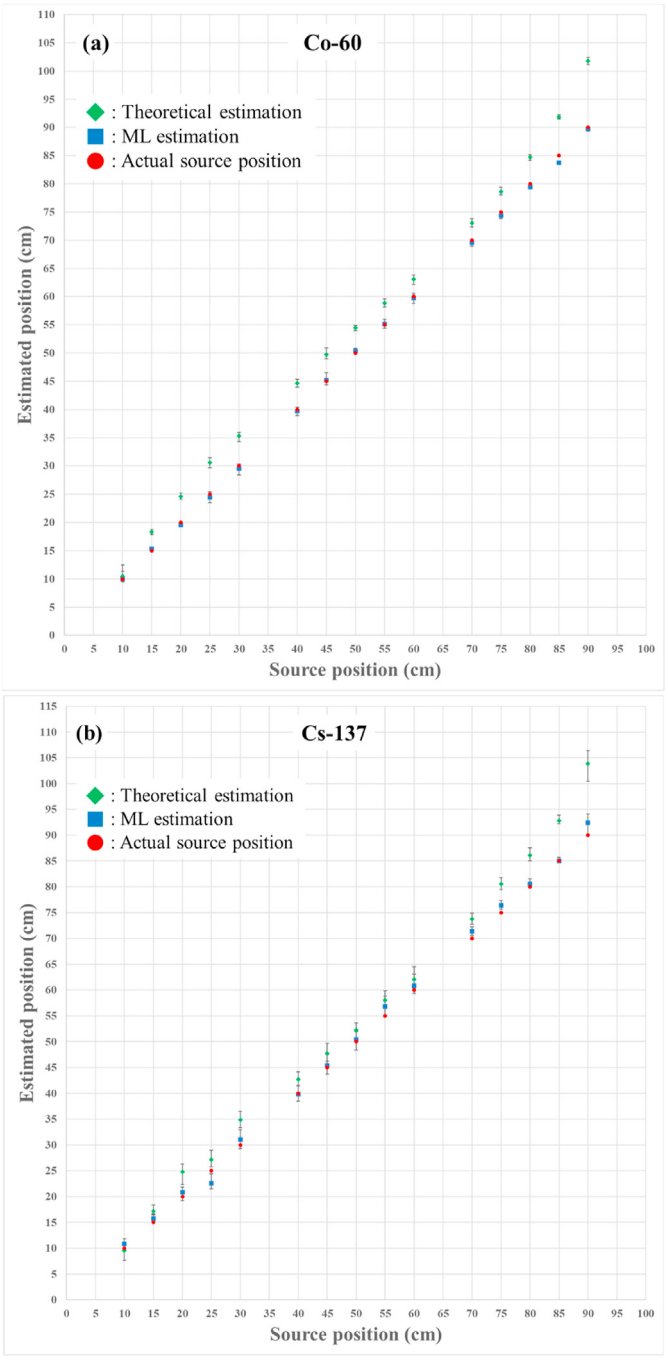

Fig. 4. ML model evaluation results for (a) Co-60 model, (b) Cs-137 model.

nine positions. The evaluation results of which are summarized in Figs. 5 and 6. Table 6 lists evaluation results in the perspective of overall error value corresponding to each ML models, and Fig. 7 shows the error plots with the cases listed in Table 6 for both radioactive sources. As shown in Fig. 7 and Table 6, the original position estimation models using every training data measured at nine positions show the lowest overall error values for both Co-60 and Cs-137 radioactive sources.

4. Conclusion

In this study, the 1D gamma ray source position is estimated using a 1 m length PSOF, two photon counters and via ML data

Fig. 5. ML model position estimation error plots for (a) Co-60 model, (b) Cs-137 model.

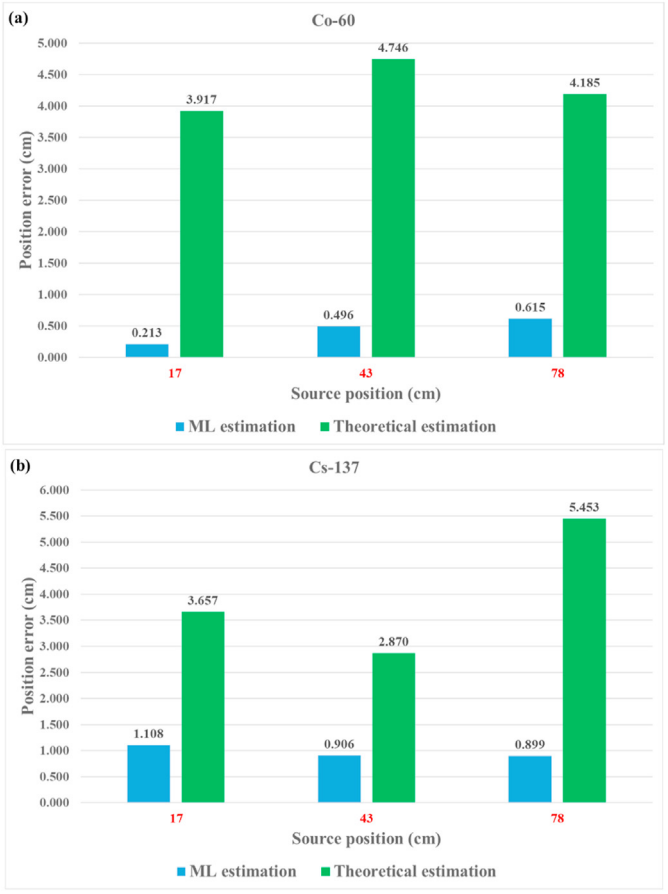

Fig. 6. Random position estimation results for (a) Co-60 model, (b) Cs-137 model.

Table 4
Estimated average positions and their standard deviations using ML and theoretical models.

Actual source position [cm]	ML estimation		Theoretical estimation	
	Average position [cm]	Standard deviation [cm]	Average position [cm]	Standard deviation [cm]
(a) Co-60				
10	10.03	0.497	10.46	0.738
15	15.37	0.174	18.37	0.256
20	19.62	0.238	24.60	0.347
25	24.44	0.642	30.58	0.595
30	29.56	0.698	35.31	0.644
40	39.69	0.413	44.64	0.380
45	45.22	0.614	49.72	0.564
50	50.37	0.309	54.46	0.284
55	55.18	0.562	58.88	0.517
60	59.74	0.543	63.08	0.501
70	69.55	0.412	73.08	0.474
75	74.36	0.393	78.64	0.455
80	79.47	0.210	84.76	0.341
85	83.77	0.145	91.83	0.241
90	89.73	0.216	101.80	0.365
(b) Cs-137				
10	10.86	0.497	9.52	0.738
15	15.83	0.174	17.19	0.256
20	20.82	0.238	24.76	0.347
25	22.60	0.642	27.14	0.595
30	31.04	0.698	34.89	0.644
40	39.79	0.413	42.74	0.380
45	45.41	0.614	47.78	0.564
50	50.39	0.309	52.24	0.284
55	56.85	0.562	58.03	0.517
60	60.85	0.543	62.10	0.501
70	71.37	0.412	73.76	0.474
75	76.45	0.393	80.53	0.455
80	80.52	0.210	86.10	0.341
85	85.07	0.145	92.84	0.241
90	92.42	0.216	103.84	0.365

Table 5
Overall error values of theoretical position estimations and ML position estimations for Co-60 and Cs-137 radioactive sources.

	ML estimation (cm)	Theoretical estimation (cm)
Co-60	0.39	4.61
Cs-137	0.97	4.24

Table 6
Training data combinations and error values for test results of (a) Co-60, (b) Cs-137 source.

Model number	Used position (cm)	Overall error (cm)
	(a) Co-60	
1	10, 50, 90	1.90
2	10, 30, 50, 70, 90	0.93
3	10, 20, 30, 40, 50, 60, 70, 80, 90	0.39
	(b) Cs-137	
1	10, 50, 90	1.85
2	10, 30, 50, 70, 90	1.64
3	10, 20, 30, 40, 50, 60, 70, 80, 90	0.97

processing. The ML training data used 1620 photon counting data at nine source positions between 10 and 90 cm. The test data used included 180 photon counting data at 18 source positions.

Various ML models are evaluated under different conditions, and the results obtained were compared with the theoretical estimations. The ML models using the data where the position is from 10 to 90 cm with 10 cm interval are determined to provide the lowest overall errors on both Co-60 and Cs-137 sources, and the IR in position estimation is 91.54% for the Co-60 source and 77.12% for the Cs-137 source.

Further studies will be conducted on the position estimation of gamma ray sources with 10 m or longer lengths and more complex shapes of PSOF using ML, in which accurate theoretical position estimation will be very difficult. In addition, nuclide identification with various kinds of PSOFs using ML spectrum analysis will be conducted in a future study to overcome one of the main disadvantageous characteristics of PSOF that finding photoelectric peak, which is considered as the most prevalent nuclide identification strategy, is impossible with PSOFs since the most dominant interaction of PSOFs and gamma ray is Compton scattering [26].

The proposed 1D gamma ray source position estimation system can be used as a radioactive leakage scanner at disposal sites with

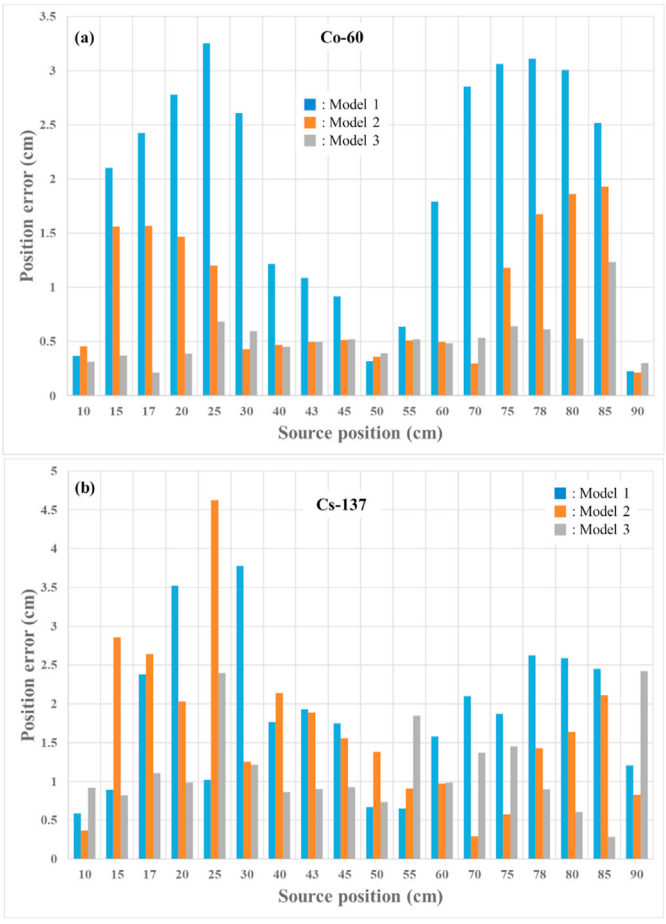

Fig. 7. Position estimation error plots of ML models using various training data for (a) Co-60, (b) Cs-137 source.

several advantageous features such as low cost, fast scanning speed and ease of maintenance.

Declaration of competing interest

The authors declare that they have no known competing financial interests or personal relationships that could have appeared to influence the work reported in this paper.

Acknowledgements

This research was supported by the Chung-Ang University Graduate Research Scholarship in 2019 and the National Research Foundation of Korea (NRF) grant funded by the Korean government (MSIT) (No. 2020M2D2A2062457).

References

[1] P. Finocchiaro, DMNR: a new concept for real-time online monitoring of short and medium term radioactive waste, in: Radioactive Waste: Sources, Types and Management; Satoshi Yuan, Wenxu Hidaka, Nova Science Publishers, Inc., New York, USA, 2012, pp. 1–40 (Chapter 1).
[2] Classification of Radioactive Waste, IAEA Safety Series No. 111-G-1.1.
[3] A. Pappalardo, C. Cali, L. Cosentino, M. Barbagallo, G. Guardo, P. Litrico, S. Scire, C. Scire, P. Finocchiaro, Performance evaluation of SiPM's for low threshold gamma detection, Nucl. Phys. B-Proc. Sup. 215 (2011) 41–43.
[4] L. Cosentino, C. Cali, G.D. Luca, G. Guardo, P. Litrico, A. Pappalardo, M. Piscopo, C. Scire, S. Scire, G. Vecchio, E. Botta, P. Finocchiaro, Real-time online monitoring of radwaste storage: a proof-of-principle test prototype, IEEE Trans. Nucl. Sci. 59 (2012) 1426–1431.
[5] G.F. Knoll, in: Radiation Detection and Measurement, fourth ed., John Wiley & Sons, Inc., New York, USA, 2010.
[6] S.D. Lee, Plastic Scintillation Fibers for Radiological Contamination Surveys; EPA/600/R-17/370, 2017.
[7] J.W. Park, G.H. Kim, Detection of gamma rays using plastic scintillating fibers, J. Nucl. Sci. Technol. 41 (2014) 373–376, sup4.
[8] A. Nohtomi, N. Sugiura, T. Itoh, T. Torii, On-line evaluation of spatial dose-distribution by using a 15-m-long plastic scintillation-fiber detector, IEEE Nuclear Science Symposium Conference Record, Dresden, Germany 19–25 (2008) 965–966.
[9] S. Soramoto, M. Notani, Y. Fukano, S. Imai, T. Iguchi, M. Zakazawa, A study of distributed radiation sensing method using plastic scintillation fiber, in: Proceeding of the 7th Workshop on Radiation Detectors and Their Uses, Tsukuba, Japan, vols. 26–27, 1993, pp. 171–172.
[10] T. Emoto, T. Trorii, T. Nozaki, H. Ando, Measurement of spatial dose-rate distribution using a position sensitive detector, Proceeding of the 8th workshop on Radiation Detectors and Their Uses 25–27 (1994) 119–121.
[11] D.L. Chichester, S.M. Watson, J.T. Johnson, Comparison of BCF-10, BCF-12, and BCF-20 scintillation fiber use in a 1-dimensional linear sensor, in: IEEE Nuclear Science Symposium and Medical Imaging Conference Record, Anaheim, CA, USA, 29 October – 3 November, 2012, pp. 365–369.
[12] H. Gamo, M. Kondo, T. Hashimoto, R. Yayama, T. Tsukiyama, Development of a PSF-detector for contaminated areas, Prog. Nucl. Energy 4 (2014) 695–698.
[13] H.H. Saito, M. Sutton, P. Zhao, E. Swanberg, Review of Decontamination Progress Surveying Technologies for Wide-Area Radiological Contamination, Lawrence Livermore National Security, Livermore, Ca., USA, 2019.
[14] S. Imai, S. Soramoto, K. Mochiki, T. Iguchi, M. Nakazawa, New radiation detector of plastic scintillation fiber, Rev. Sci. Instrum. 62 (1991) 1093–1096.
[15] C. Whittaker, C.A.G. Kalnins, D. Ottaway, N.A. Spooner, H. Ebendorff-Heidepriem, Transmission loss measurements of plastic scintillating optical fibres, Opt. Mater. Express 9 (2019) 1–12.
[16] K.K. Hamamatsu Photonics, Photon counting head H11890 series datasheet, Available online: https://www.hamamatsu.com/resources/pdf/etd/H11890_TPMO1052E.pdf.
[17] M. Rupali, P. Amit, A review paper on general concepts of "Artificial intelligence and machine learning", IARJSET 4 (2017) 79–82.
[18] S.J. Russell, P. Norvig, in: Artificial Intelligence: A Modern Approach, fourth ed., Prentice Hall, NJ, USA, 2020.
[19] F. Chollet, Deep Learning with Python, Manning Publications, Inc.: Shelter Island, NY, USA, 2017.
[20] R.G. Peyvandi, S.Z. Islami Rad, Application of artificial neural networks for the prediction of volume fraction using spectra of gamma rays backscattered by three-phase flows, Eur. Phys. J. Plus. 132 (2017) 511.
[21] R.G. Peyvandi, S.Z. Islami Rad, Precise prediction of radiation interaction position in plastic rod scintillators using a fast and simple technique: artificial neural network, Nucl. Eng. Technol. 50 (2018) 1154–1159.
[22] Saint-Gobain Crystals, Plastic scintillating fibers product sheet, Available online: https://www.crystals.saint-gobain.com/sites/imdf.crystals.com/files/documents/fiber-product-sheet.pdf.
[23] D.F. Swinehart, The beer-lambert law, J. Chem. Educ. 39 (1962) 333.
[24] A.F.M. Agarap, Deep learning using rectified linear units (ReLU), Available online: arxiv.org/pdf/1803.08375.
[25] D.P. Kingma, J.L. Ba, Adam: a method for stochastic optimization, in: 3rd International Conference for Learning Representations, San Diego, 2015. Available online: arxiv.org/pdf/1412.6980.
[26] Shi-Biao Tang, Qing-Li Ma, Ze-Jie Yin, H. Huang, Simulation study on detection efficiency of plastic scintillating fiber under γ-ray radiation, Radiat. Phys. Chem. 77 (2008) 115–120.